Chemical Physics Letters 650 (2016) 130–137

Contents lists available at ScienceDirect

Chemical Physics Letters

journal homepage: www.elsevier.com/locate/cplett

Low-pressure equilibrium binary argon–methane gas mixture adsorption on exfoliated graphite: Experiments and simulations

Alberto Albesa[a], Brice Russell[b], José Luis Vicente[a], Matías Rafti[a,*]

[a] Instituto de Investigaciones Fisicoquímicas Teóricas y Aplicadas (INIFTA), Universidad Nacional de La Plata-CONICET, CC. 16, Suc. 4, 1900 La Plata Argentina
[b] Department of Physics, Southern Illinois University, Carbondale, IL 62901, United States

ARTICLE INFO

Article history:
Received 17 December 2015
In final form 29 February 2016
Available online 5 March 2016

ABSTRACT

Adsorption equilibrium measurements of pure methane, pure argon, and binary mixtures over exfoliated graphite were carried for different initial compositions, temperatures, and total pressures in the range of 0.1–1.5 Torr using the volumetric static method. Diagrams for gas and adsorbed phase compositions were constructed for the conditions explored, and isosteric heats of adsorption were calculated. Experimental results were compared with predictions obtained with Monte Carlo simulations and using the Ideal Adsorbed Solution Theory (IAST).

1. Introduction

Adsorption of technologically relevant gas mixtures over different porous solid materials, constitutes a research topic of great interest due to its potential use for separation, storage, and purification applications [1–5]. While industrial scale separations are carried mainly via distillation; an increasing number of applications make use of the far less energy-consuming adsorption-based techniques. Adsorbents used for these purposes include both, classic materials such as activated carbons (AC) and zeolites, and novel porous materials belonging to the family of Microporous Coordination Polymers (also known as Metal Organic Frameworks or MOFs) [6,7]. Among the most archetypal study cases, CO_2 separation from methane or nitrogen mixtures, and olefin/paraffin separations can be mentioned [8–15].

The problem of differential adsorption of components from a gas mixture was usually tackled in the literature from the specific industrial application perspective; i.e., with experiments conducted on high-pressure regimes [16–18]. There are two approaches for the study of gas mixtures adsorption; the so-called static volumetric method, and the breakthrough or dynamic method. For the static volumetric method, adsorbate gas-mixture (with a predefined initial molar composition) is allowed into the measurement cell, where the adsorbent is contained, up to a given total initial pressure. As a result of the adsorption process, the total pressure would asymptotically decrease toward an equilibrium final value; in order avoid this and to keep total pressure constant throughout the process, some experimental setups allow for compensation via controlled volume reduction [19,20]. On the other hand, breakthrough methods are carried by allowing a constant composition/pressure adsorbate gas mixture flux through an adsorbent-bed, while the effluent composition versus time is recorded. Dynamic methods require operation under relatively high mass flows and pressures, thus the pressure ranges below 10 Pa are not accessible [21–24].

Although there is a vast amount of literature dealing theoretically with problem of gas mixtures adsorption in terms of adsorbate–adsorbate and adsorbate–adsorbent interactions [25,26], a complete understanding of the processes leading to preferential adsorption is still lacking. It is in this context that experimental studies exploring the low-pressure regime become necessary. For example, Rawat et al. [27] predicted recently from Monte Carlo simulations, a so-called overshoot effect (a kinetically-driven selectivity reversal) that occurs in the early stages of adsorption of binary gas mixtures. This effect consists in the appearing of a local minimum in surface coverage of the strong binding component, instead of the expected monotonic increase toward its final equilibrium value; weak-binding species coverage also displays a local maximum (hence the name overshoot). This effect was experimentally confirmed for argon–methane mixtures adsorption over exfoliated graphite [28]. Most of the current interest in adsorption from gas-mixtures has been focused on new nanostructured adsorbent materials such as metal-organic frameworks (MOFs) or carbon nanotubes (CNT) [6,29,30]. However, the lack of complete information regarding the simplest adsorbates over the most commonly studied adsorbents (e.g., exfoliated

* Corresponding author.
E-mail address: mrafti@quimica.unlp.edu.ar (M. Rafti).

http://dx.doi.org/10.1016/j.cplett.2016.02.070
0009-2614/

graphite) prompts the need of further basic experimental studies using such materials. This is the task that we undertake in the present study.

Taking into account the above discussed motivations, we performed gas adsorption experiments of pure Ar, pure CH_4, and several binary mixtures, over exfoliated graphite. Using the static volumetric method for different temperatures, we constructed diagrams for compositions of gas phase vs. adsorbed phase. In order to test the predictive power of commonly used theoretical tools in multicomponent equilibrium adsorption, experiments were compared with results obtained both using the Ideal Adsorbed Solution Theory (IAST) [31] and performing Monte Carlo simulations on the Grand Canonical ensemble (GCMC). The two above mentioned calculation methods can be best compared when applied to systems that fulfill basic assumptions of IAST (although the range of applicability can be extended by introducing non-ideality, as recently demonstrated by Furmaniak et al. [32]); i.e., weakly interacting mixture components, low surface coverages, and quasi-homogeneous adsorbent. The hereby studied system (Ar/CH_4 mixtures adsorption over exfoliated graphite) features the above mentioned characteristics: adsorbate molecules can be approximately described as spherical weakly-interacting species adsorbing on a planar, non-porous surface with homogeneous adsorption energy distribution [33].

2. Materials and methods

2.1. Experimental details

Adsorption measurements with binary argon–methane mixtures were conducted on exfoliated graphite in the 0.1–1.5 Torr pressure range for different final total pressures at two temperatures using the volumetric static method (mass of adsorbent sample 0.2165 g, and research grade Matheson gases with purity 99.9995%). Our in-house built experimental setup allows for temperature control over the range 20–300 K, and gas phase composition analysis through the use of a differentially pumped Quadrupole Mass Spectrometer residual gas analyzer (QMS-RGA), which is connected to the measurement cell via a finely controlled needle valve which allows for very small openings to minimize the amount of gas being removed by the turbo-molecular pump. In this way equilibrium state attained by the system remains unperturbed during gas phase composition measurements (see, e.g., Ref. [34] for detailed description of the setup).

In order to map the system behavior We explored four different values for initial pressure and three different gas phase mixture compositions (namely, 0.25:0.75, 0.50:0.50, and 0.75:0.25, Ar:CH_4 proportions), additionally to the pure components. Our experimental procedure can be summarized as follows: (i) a known amount of gas mixture is admitted into the cell containing the graphite adsorbent (the initial total pressures, $P_{tot,i}$ used were always in the range of 0.1–1.5 Torr); (ii) the gas phase composition is determined as it changes in the initial stages (during the first 1000 s) of the adsorption process by opening the needle valve which connects the measurement cell to the QMS-RGA (the valve was opened in such way that pressure in the QMS never rises above 5×10^{-8} mbar, thus ensuring that perturbation of the system as a result of mass loss is negligible during this time period); (iii) the total pressure decrease due to adsorption is monitored continuously, from the moment in which the gas is admitted into the cell until equilibrium is attained, at this point the total final pressure ($P_{tot,f}$), and final composition are recorded; (iv) the cell is brought to room temperature and the sample is evacuated at ambient temperature; then steps (i) to (iii) are repeated for a new value of the initial pressure, $P_{tot,i}$; (v) after completion of experiments for all four initial pressure values, steps (i) to (iv) were repeated for the new initial gas mixture composition. Using measured values for final total pressure, final gas phase composition, and the corresponding final adsorbed phase composition, the following diagrams were constructed for every (T, $P_{tot,f}$) parameter pair explored: (i) Y_1 vs. X_1 (where 1 = Argon, 2 = Methane, and X and Y stand for molar fractions in the adsorbed phase, and in the gas phase respectively); (ii) N_{ads}, N_1 and N_2 vs. Y_1 (where N_{ads} is the total amount of gas adsorbed and N_1 and N_2 are the total amounts of argon or methane initially admitted into the system).

Table 1
Parameters used in the experiments.

Temperature (K)	$P_{tot,f}$ (Torr)	Initial gas phase composition (CH_4:Ar)
84	0.31	1.00:0.00
	0.57	0.75:0.25
	1.35	0.50:0.50
		0.25:0.75
		0.00:1.00
94		1.00:0.00
	1.04	0.75:0.25
		0.50:0.50
		0.25:0.75
		0.00:1.00

In each individual measurement (i.e., for each dose of gas mixture admitted into the cell) the time that we allowed for the system to attain equilibrium was 24 h. Adsorption isotherms of pure gases were used to obtain isosteric heats and approximate monolayer completion values. The gas mixtures were prepared in a volume attached to the dosing volume using ultra-high purity gases, and the amount of mixture prepared was calculated in such way that it was enough for the whole set of experiments (two temperatures and 4 different final equilibrium pressures). Table 1 summarizes the parameter values explored. It should be noted that $P_{tot,f}$ values obtained depend on both $P_{tot,i}$ and on the initial composition [35]. In order to establish meaningful comparisons for the entire data set, we used the equilibrium $P_{tot,f}$ value obtained in the first round of experiments for the complete set of compositions tested. That is to say, if the first round of experiments was performed using (0.75:0.25) Ar–CH_4 mixture, and for an initial pressure $P_{tot,i}$ = 1.50 Torr used, yielded a $P_{tot,f}$ = 0.50 Torr value, then the experiments carried using the remaining compositions were performed in such way that a $P_{tot,f}$ = 0.50 Torr was also obtained for the sake of the validity of comparisons made. This is not a trivial task because of the above mentioned dependence on the gas mixture composition used. In order to solve this problem, multiple experiments with slightly different initial total pressures were carried for each composition. Typically, values above and below the targeted equilibrium $P_{tot,f}$ value were obtained. These values were then used to obtain, via linear interpolation, the results for the desired targeted final pressure value.

2.2. Monte Carlo simulations details

We have considered for all the simulations presented in this letter the pairwise interaction potential between Ar and CH_4 as described by the 1-center Lennard–Jones (LJ) model. The LJ parameters used in the simulations are listed in Table 2. The potential

Table 2
Lennard–Jones interaction parameters.

	$\varepsilon_{XX/kB}$	$\sigma_{XX/Å}$
CH_4 (X=f)	148.1	3.81
Ar (X=f)	117.5	3.405
Graphite (X=s)	28	3.40

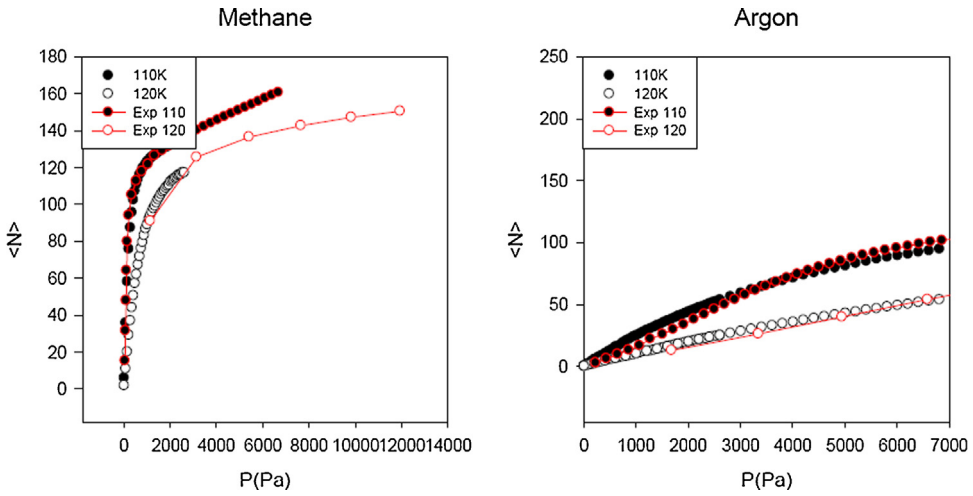

Figure 1. Experimental and simulated: (a) methane and (b) argon isotherms at 110 K and 120 K temperature.

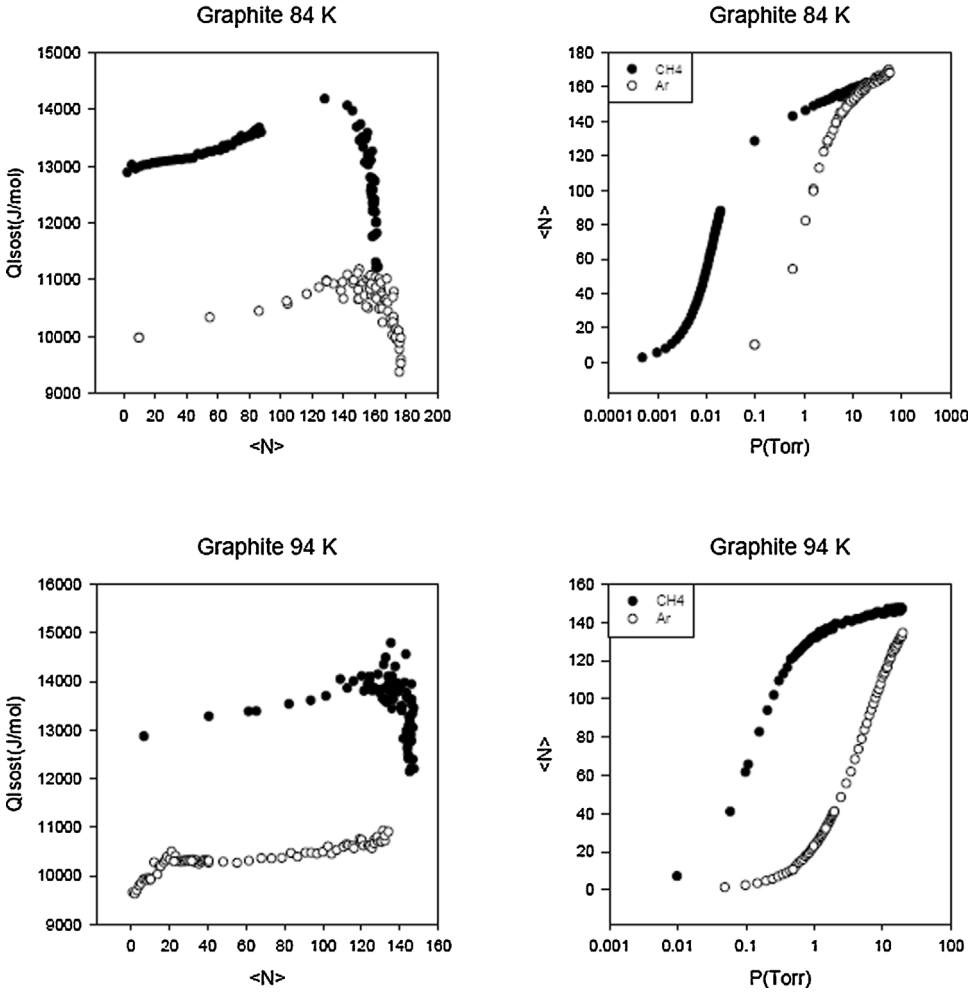

Figure 2. (right column) Isotherms for pure components in the region explored within the mixture adsorption measurements and (left column) determined isosteric heats of adsorption (behavior for wider temperature range used for isosteric heat calculation is presented in Sup. Inf.).

energy of interaction between two fluid particles was calculated using the LJ 12-6, as described in the following equation:

$$U_{ff}(r) = 4\varepsilon_{ff}\left[\left(\frac{\sigma_{ff}}{r}\right)^{12} - \left(\frac{\sigma_{ff}}{r}\right)^{6}\right] \quad (1)$$

where r is the separation distance between the two particles. The interaction energy between a fluid particle and a carbon atom was calculated using the same equation, Eq. (1), with σ_{ff} and ε_{ff} being replaced by σ_{sf} and ε_{sf}, respectively. These cross-molecular parameters are calculated from the usual Lorentz–Berthelot rule, see Eq. (2)

$$\varepsilon_{sf} = (\varepsilon_{ss}\varepsilon_{ff})^{1/2}, \quad \sigma_{sf} = \frac{1}{2}(\sigma_{ss} + \sigma_{ff}) \tag{2}$$

Assuming that pairwise additivity holds, the total energy is calculated by summing the pairwise interactions between fluid particles, and between individual carbon atoms and fluid particles, as follows:

$$U = \sum_{i,j>i} {}_{ij}(|r_i - r_j|) + \sum_{i,k} {}_{ik}(|r_i - r_k|) \tag{3}$$

where r_i and r_j are the positions of fluid particles i and j, respectively, r_k is that of a carbon atom, φ_{ij} is the pair interaction potential energy between fluid particles, and φ_{ik} is that between particle i and carbon atom k.

2.3. Isosteric heat of adsorption calculations

The isosteric heat of adsorption for the ith component of an ideal gas mixture ($q_{st,i}$), can be calculated using the following expression:

$$\frac{q_{st,i}}{RT^2} = \left[\frac{d \ln p_i}{dT}\right]_{n_i} \tag{4}$$

where $p_i = P\,y_i$ stands for the partial pressure of the ith component (P and y_i are total gas pressure and molar fraction in gas phase) in equilibrium with n_i moles in the adsorbed phase, T is the temperature; and R is the gas constant. However, Eq. (4) is not a practical method for calculating the isosteric heat because the data required are rarely found in the literature. In Monte Carlo simulations the isosteric heat can be calculated from

$$q_{st,i} = (H^b - H^{*,b}) + RT - \left(\frac{\partial U^{a,c}}{\partial N^a}\right)_{T,V^a} \tag{5}$$

where the superscripts a, b, and * respectively denote the value of the thermodynamic functions for the adsorbed, gas and ideal phases. $U^{a,c}$ is the configurational part of the interaction energy, which includes both adsorbate–adsorbate and adsorbate–adsorbent interactions. Assuming that the gas behaves as an ideal gas, Eq. (5) becomes:

$$q_{st,i} = RT - \left(\frac{\partial U^{a,c}}{\partial N^a}\right)_{T,V^a} \tag{6}$$

Here $\partial U^{a,c}/\partial N$ can be obtained either by numerical differentiation or from fluctuation theory:

$$\left(\frac{\partial U^{a,c}}{\partial N^a}\right) = \frac{f(U,N)}{f(N,N)} \quad \text{where} \quad f(X,Y) = \langle XY\rangle - \langle X\rangle\langle Y\rangle \tag{7}$$

Here the brackets, $\langle X\rangle$ indicate the mean value of the quantity X. The heat of adsorption of the ith component of a binary mixture can be obtained from the simulations solving the following expressions:

$$q_{st,i} = RT - \left(\frac{\partial U^{a,c}}{\partial N_i^a}\right)_{T,V^a,N^a_{j\neq i}} \tag{8}$$

$$\left(\frac{\partial U^{a,c}}{\partial N^a}\right) = \sum_k \left(\frac{\partial U^{a,c}}{\partial \beta\mu_k}\right)_{T,V^a,N^a_{j\neq i}} \left(\frac{\partial \beta\mu_k}{\partial N_i^a}\right)_{T,V^a,N^a_{j\neq i}} \tag{9}$$

where

$$\left(\frac{\partial U^{a,c}}{\partial \beta\mu_k}\right)_{T,V^a,N^a_{j\neq i}} = f(U, N_k^a) \tag{10}$$

$$\begin{pmatrix} \frac{\partial \beta\mu_1}{\partial U_1^a} & \frac{\partial \beta\mu_1}{\partial U_2^a} \\ \frac{\partial \beta\mu_2}{\partial U_1^a} & \frac{\partial \beta\mu_2}{\partial U_2^a} \end{pmatrix} = \begin{pmatrix} f(N_1^a, N_1^a) & f(N_1^a, N_2^a) \\ f(N_2^a, N_1^a) & f(N_2^a, N_2^a) \end{pmatrix}^{-1} \tag{11}$$

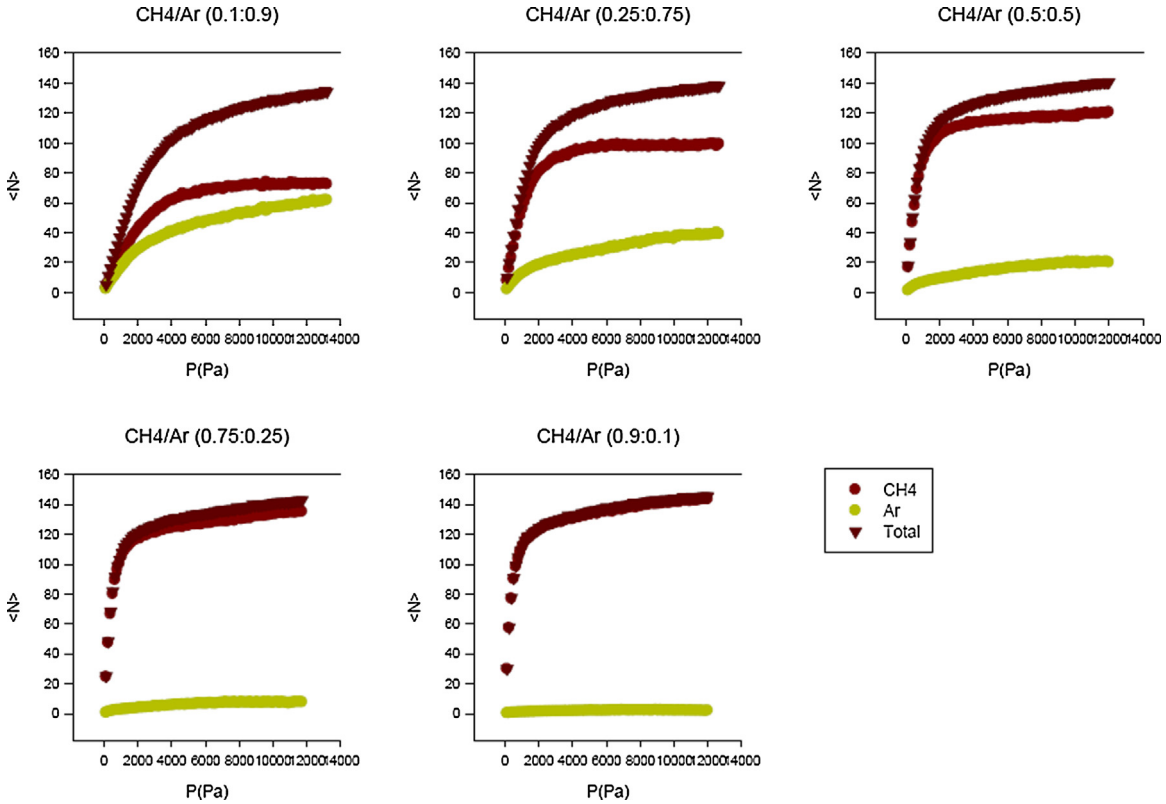

Figure 3. Simulations for adsorption from mixtures of methane and argon at $T = 110$ K with different gas phase composition CH_4:Ar: (a) 0.1:0.9, (b) 0.25:0.75, (c) 0.5:0.5, (d) 0.75:0.25, and (e) 0.9:0.1.

Table 3
Isosteric heats (Q_{st}) (values reported by Cole et al. also presented for comparison).

Species	Q_{st} (kJ/mol) This work	Q_{st} (kJ/mol) From ref. [36]
Methane	12.2	12.16
Argon	9.5	9.55

The isosteric heat of adsorption of the components of a gas mixture is a helpful quantity for understanding the selectivity of a given adsorbent. The selectivity $S_{i,j}$ of the ith species relative to the jth species can be defined as follows:

$$S_{i,j} = \frac{\theta_i/\theta_j}{p_i/p_j}. \tag{12}$$

Here θ_i and θ_j are loading for species i and j and p_i and p_j the corresponding partial pressures.

2.4. The Ideal Adsorbed Solution Theory (IAST)

The Ideal Adsorbed Solution Theory (IAST) was developed originally by Myers and Prausnitz [31] and is widely used to predict mixtures adsorption from data of the pure components. The IAST is analog to Raoult's Law for vapor-liquid equilibrium and assumes that the adsorbed mixture is an ideal solution. Therefore, for a component i in an ideal solution with mole fraction x_i, it follows that:

$$p_i = p_i^0(\pi)x_i \tag{18}$$

where p_i is the partial pressure of component i and $p_i^0(\pi)$ is the pressure of the pure component i at the same spreading pressure π of the mixture. The spreading pressure per unit area is related to p_i^0 by the Gibbs adsorption isotherm:

$$\pi = RT \int_0^{p_i^0} n_i(p) d\ln p \tag{19}$$

where $n_i(p)$ is the adsorption isotherm of pure component i given by any isotherm that fits well with the experimental data. The amount of gas adsorbed can be calculated by the expression:

$$n_{i,m} = \frac{x_i}{\sum_k x_k/n_k^0(p_k^0)} \tag{20}$$

At a given pressure and composition Eqs. (18)–(20) can be solved, together with the identity:

$$\sum_i \frac{p_{i0}}{p_i^0(\pi)} = 1 \tag{21}$$

to obtain the adsorbed amount of the individual components in a mixture.

The set of equations presented cannot, generally, be solved analytically and therefore must be solved numerically, although the spreading pressure can be calculated analytically for the Sips isotherm. The Sips isotherm is an empirical isotherm that satisfies the limits of low and high pressures. It is useful for describing systems at sub-monolayer coverages and has the following form.

$$n_i = n_{\max} \frac{(bp)^{1/n}}{1 + (bp)^{1/n}} \tag{22}$$

The parameters $n_{\max}$, n and b are characteristic of each adsorbate–adsorbent system. The more the parameter n becomes different from $n = 1$, the more heterogeneous the system under study is.

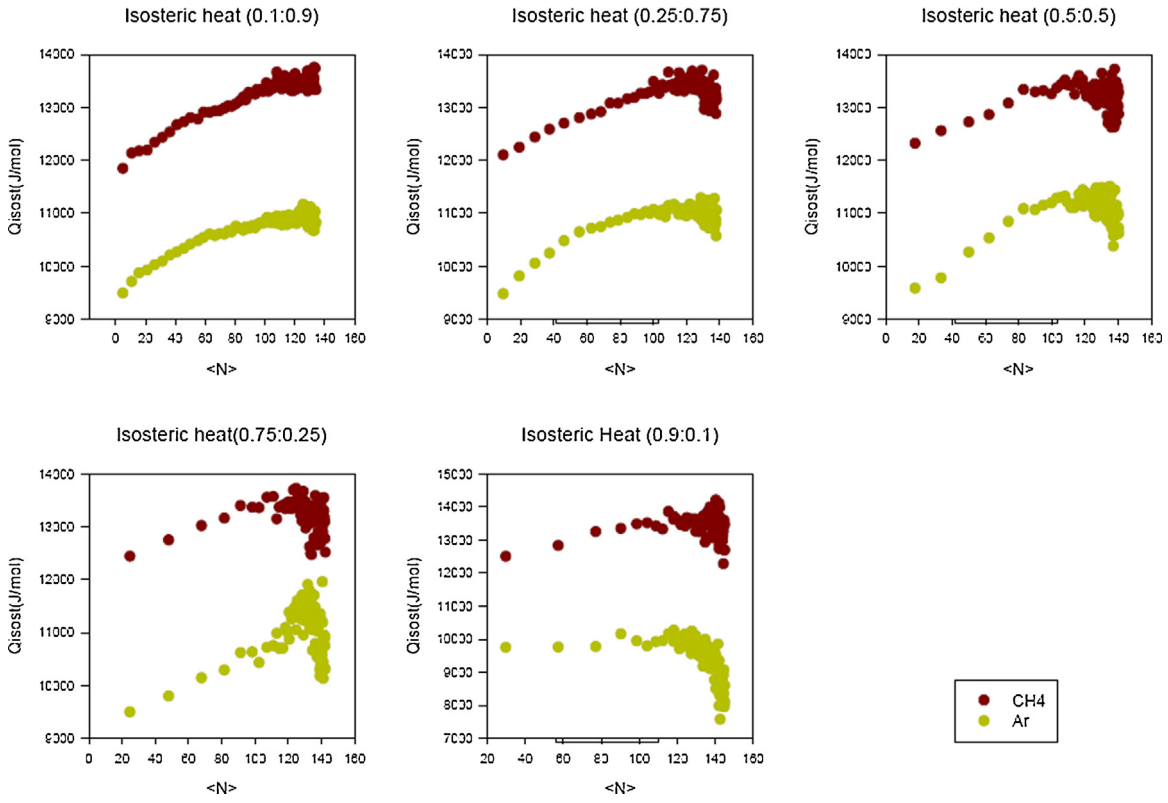

Figure 4. Isosteric heats calculated for Ar (light green) and CH_4 (dark brown) as a function of total coverage at $T = 110$ K with different gas phase composition CH_4:Ar: (a) 0.1:0.9, (b) 0.25:0.75, (c) 0.5:0.5, (d) 0.75:0.25, and (e) 0.9:0.1. (For interpretation of the references to color in this figure legend, the reader is referred to the web version of this article.)

3. Results and discussion

3.1. Adsorption experiments and simulations for pure gases

Adsorption experiments and simulations for pure gases over exfoliated graphite were compared in order to test the accuracy and suitability of the methods described in previous section, results of such comparison are presented in Figure 1.

Valuable information for understanding the behavior of the gas mixtures can be extracted from pure component isotherms. In particular we can determine the isosteric heat of adsorption (Q_{st}). Figure 2 shows the isotherms in logarithmic scale and the isosteric heat of adsorption for the pure component gases, while Table 2 displays numerical isosteric heat values obtained. The logarithmic plot in Figure 3b is directly related to chemical potential. In such a plot, different binding energy sites will appear as sub-steps in the isotherm. Clearly, in the range of pressures in which the monolayer is completed, only one rounded sub-step is present, as is to be expected for the adsorbent used. Good agreement with previously reported isosteric heats was obtained as can be observed in Table 3, where Q_{st} values corresponding to zero coverage limit are presented [36]. These two species have sufficiently different binding energies on graphite as to enable us attempt the detection of selective adsorption.

The complete set of calculated Sips parameters of the pure component isotherms are shown in supplementary information. These results show that the energy related term b is much higher in Methane isotherms than in argon isotherms, as was expected. The heterogeneity parameter n is close to one.

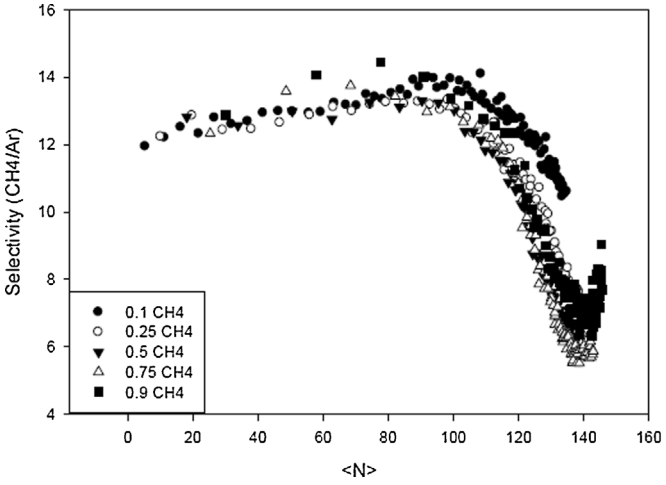

Figure 5. Selectivity calculated as a function of the number of adsorbed molecules, according to the simulations performed.

3.2. Simulations for binary mixtures adsorption

Simulation results obtained for adsorption of CH_4 and Ar mixtures performed at $T = 110$ K with different gas phase compositions can be observed in Figure 3. As was the case for the single-component isotherms, more methane than argon adsorbs on graphite in all cases for the same pressure. Once the 'knee' of the isotherm is reached, (when the number of molecules is approx. 120,

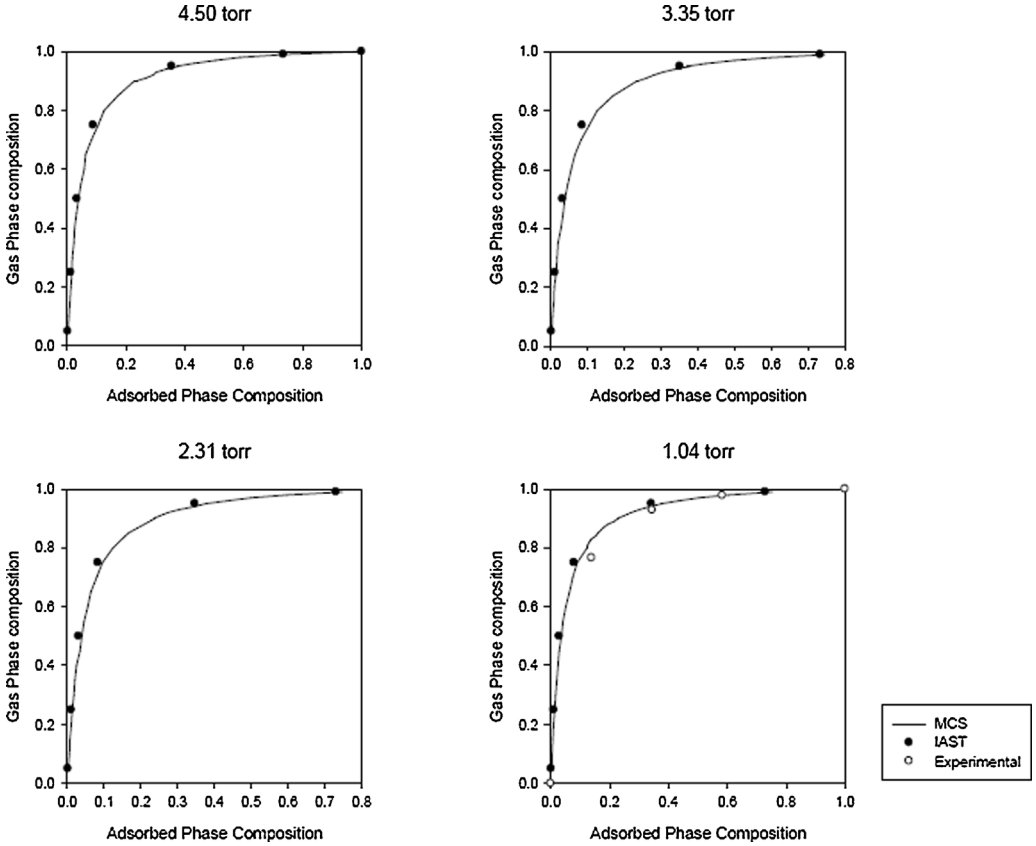

Figure 6. MC simulations (lines) and IAST (filled circles) comparison for the dependence between adsorbed and gas phase compositions of CH_4 and argon mixtures over graphite at 94 K. Experimentally determined values (open circles) are also included in the diagrams for the explored compositions.

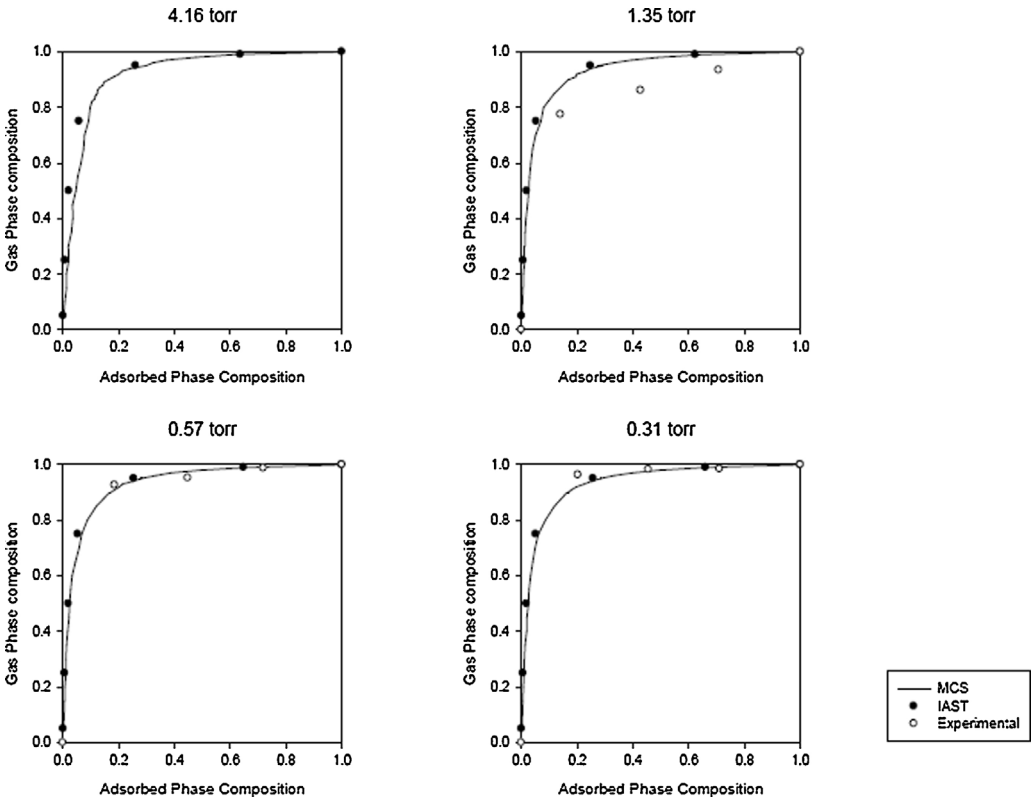

Figure 7. MC simulations (lines) and IAST (filled circles) comparison for the dependence between adsorbed and gas phase compositions of CH_4 and argon mixtures over graphite at 84 K. Experimentally determined values (open circles) are also included in the diagrams for the explored compositions.

i.e., at coverage 0.7) the number of adsorbed methane molecules remain almost constant, and the rate of argon adsorption increases.

Figure 4 shows the isosteric heats determined for Ar and CH_4 as a function of total loading corresponding to the conditions described in Figure 3. The isosteric heat of Ar and CH_4 correspond to the values of pure gases.

Figure 5 shows the selectivity as a function of the number of adsorbed molecules. It can be seen that the selectivity is mainly a function of the adsorbed amount and not of gas phase composition. The selectivity drops when the coverage is about 0.7 and reaches its minimum when the monolayer is complete, then it rises again.

3.3. Comparison of IAST calculations and Monte Carlo simulations with experimental data on binary mixtures adsorption

Diagrams obtained from Monte Carlo (MC) simulations and IAST calculations for the variation of gas phase composition vs. adsorbed phase composition are presented in Figures 6 and 7. The agreement reached for a wide range of total pressures explored, ensures the suitability of the simulation method (see Supp. Inf. for additional temperatures explored). Experiments were carried for mixtures corresponding to the pressures and compositions listed in Table 1, at 84 K and 94 K temperatures. The results obtained were included in the corresponding diagrams, which are presented also in Figures 6 and 7.

Experiments in which total pressure P_{Tot} values were increased for $T = 84$ K show that the adsorbed phase in equilibrium becomes increasingly richer in Ar, as can be observed in Figure 7. Comparing the available P_{tot} measurement for $T = 94$ K with similar range for $T = 84$ K, shows both, a less Ar-rich adlayer, together with better agreement of experiments and ideal behavior, as can be observed for 1.04 Torr total pressure in Figure 6. This effect can be understood by considering the higher binding energy of CH_4 on exfoliated graphite; due to its lower binding energy, argon requires higher pressures to form denser adlayers, thus the trend observed for a given temperature (see also additional simulation results for 100 K and 110 K temperatures in Sup. Inf.). The results obtained using IAST and MC simulations are considerably in line with experimental observations (e.g., no azeotrope was found according to theoretical predictions), which allows to speculate on a quasi-ideal mixture behavior. As total pressure values used increase, the behavior deviates from predictions, as can be observed in Figure 7, $P_{tot} = 1.35$ Torr.

4. Conclusions

We have performed experiments for the adsorption of Ar–CH_4 gas mixtures at different compositions and temperatures using the static volumetric approach. The low pressure–low coverages values used allowed us to compare the experimental results with numerical Monte Carlo simulations, and to assess the influence of the adsorbate–adsorbate/adsorbate–adsorbent interaction on the agreement obtained.

Using pure data isotherms and mixtures adsorption, we compared the experimental results with the IAST predictions in order to determine whether the system could be considered ideal or not in the parameter range studied. Conditions for ideal behavior depend on (i) ratio of the isotherm temperature and the critical temperature for the adsorbate and (ii) pressures used and difference between binding energies of the adsorbates on the adsorbent surface.

The selectivity trends observed can be understood by taking into account that selective adsorption depends on two factors, the energetic and the entropic contributions. The energetic factor is related to the enthalpy of adsorption, and the entropic factor is related to the number of possible configurations that the system can adopt. While the energetic factor is important at low pressures,

the entropic factor becomes increasingly more important at higher pressures.

Acknowledgments

The authors gratefully acknowledge financial support granted via a joint collaboration project of CONICET (Argentina) and NSF (USA). Prof. Aldo Migone (SIU, Carbondale, US) is also gratefully acknowledged for valuable discussions and help with the experimental measurements. We also thank UnCaFiQT (SNCAD) for computational resources. MR and AGB are CONICET fellows, and JLV is a fellow of CIC-PBA, Argentina.

Appendix A. Supplementary data

Supplementary data associated with this article can be found, in the online version, at doi:10.1016/j.cplett.2016.02.070.

References

[1] T. Devic, C. Serre, Ordered Porous Solids, Elsevier, 2009, http://dx.doi.org/10.1016/B978-0-444-53189-6.00004-4.
[2] K.M. Steel, W.J. Koros, Carbon 41 (2003) 253, http://dx.doi.org/10.1016/S0008-6223(02)00309-3.
[3] A.I. Fatehi, K.F. Loughlin, M.M. Hassan, Gas Sep. Purif. 9 (1995) 199, http://dx.doi.org/10.1016/0950-4214(95)98227-C.
[4] H. Zhang, P. Deria, O.K. Farha, J.T. Hupp, R.Q. Snurr, Energy Environ. Sci. 8 (2015) 1501, http://dx.doi.org/10.1039/C5EE00808E.
[5] G. Caputo, D. Mazzei, M.F. Sgroi, in: M. De Falco, A. Basile (Eds.), Enriched Methane, Springer, 2016, p. 37, http://dx.doi.org/10.1007/978-3-319-22192-2_3.
[6] J.-R. Li, J. Sculley, H.-C. Zhou, Chem. Rev. 112 (2012) 869, http://dx.doi.org/10.1021/cr200190s.
[7] J.-R. Li, R.J. Kuppler, H.-C. Zhou, Chem. Soc. Rev. 38 (2009) 1477, http://dx.doi.org/10.1039/b802426j.
[8] R.T. Yang, Gas Separation by Adsorption Processes, Elsevier, Stoneham, 1987, http://dx.doi.org/10.1016/B978-0-409-90004-0.50001-5.
[9] M. Li, E. Xu, T. Wang, J. Liu, Langmuir 28 (2012) 2582, http://dx.doi.org/10.1021/la203387h.
[10] J. McEwen, J.D. Hayman, A. Ozgur Yazaydin, Chem. Phys. 412 (2013) 72, http://dx.doi.org/10.1016/j.chemphys.2012.12.012.
[11] A. Van Miltenburg, W. Zhu, F. Kapteijn, J.A. Moulijn, Chem. Eng. Res. Des. 84 (2006) 350, http://dx.doi.org/10.1205/cherd05021.
[12] A.G. Albesa, M. Rafti, D.S. Rawat, J.L. Vicente, A.D. Migone, Langmuir 28 (2012) 1824, http://dx.doi.org/10.1021/la204314a.
[13] V. Krungleviciute, M.M. Calbi, J.A. Wagner, A.D. Migone, M. Yudasaka, S. Iijima, J. Phys. Chem. C 112 (2008) 5742, http://dx.doi.org/10.1021/jp710524q.
[14] M. Mofarahi, F. Gholipour, Microporous Mesoporous Mater. 200 (2014) 1, http://dx.doi.org/10.1016/j.micromeso.2014.08.022.
[15] L. Hamon, E. Jolimaître, G.D. Pirngruber, Ind. Eng. Chem. Res. 49 (2010) 7497, http://dx.doi.org/10.1021/ie902008g.
[16] C. Balzer, T. Wildhage, S. Braxmeier, G. Reichenauer, J.P. Olivier, Langmuir 27 (2011) 2553, http://dx.doi.org/10.1021/la104469u.
[17] M.L. Zanota, N. Heymans, F. Gilles, B.L. Su, M. Frère, G. De Weireld, J. Chem. Eng. Data 55 (2010) 448, http://dx.doi.org/10.1021/je900539m.
[18] R. Reich, W.T. Ziegler, K.A. Rogers, Ind. Eng. Chem. Process Des. Dev. 19 (1980) 336, http://dx.doi.org/10.1021/i260075a002.
[19] J.Ř. Čermáková, A. Marković, P. Uchytil, A. Seidel-Morgenstern, Chem. Eng. Sci. 63 (2008) 1586, http://dx.doi.org/10.1016/j.ces.2007.11.021.
[20] M.J. Heslop, B.A. Buffham, G. Mason, Ind. Eng. Chem. Res. 39 (2000) 1514, http://dx.doi.org/10.1021/ie990396r.
[21] Y. Belmabkhout, G. Pirngruber, E. Jolimaitre, A. Methivier, Adsorption 13 (2007) 341, http://dx.doi.org/10.1007/s10450-007-9032-6.
[22] R. Krishna, J.R. Long, J. Phys. Chem. C 115 (2011) 12941, http://dx.doi.org/10.1021/jp202203c.
[23] P. Liu, H. Zhang, H. Xiang, Y. Yan, Sep. Purif. Technol. 158 (2016) 1, http://dx.doi.org/10.1016/j.seppur.2015.12.003.
[24] M.C. Campo, A.M. Ribeiro, A.F.P. Ferreira, J.C. Santos, C. Lutz, J.M. Loureiro, et al., Fuel Process. Technol. 143 (2016) 185, http://dx.doi.org/10.1016/j.fuproc.2015.11.024.
[25] P. He, H. Liu, Y. Li, J. Zhu, S. Huang, Z. Lei, et al., Adsorption 18 (2011) 31, http://dx.doi.org/10.1007/s10450-011-9378-7.
[26] R. Babarao, J. Jiang, S.I. Sandler, Langmuir 25 (2009) 5239, http://dx.doi.org/10.1021/la803074g.
[27] D.S. Rawat, V. Krungleviciute, L. Heroux, M. Bulut, M.M. Calbi, A.D. Migone, Langmuir 24 (2008) 13465, http://dx.doi.org/10.1021/la8022002.
[28] M. Rafti, V. Krungleviciute, A.D. Migone, Chem. Phys. Lett. 554 (2012) 67, http://dx.doi.org/10.1016/j.cplett.2012.10.017.
[29] S.J. Geier, J.A. Mason, E.D. Bloch, W.L. Queen, M.R. Hudson, C.M. Brown, et al., Chem. Sci. 4 (2013) 2054, http://dx.doi.org/10.1039/c3sc00032j.
[30] E.D. Bloch, W.L. Queen, R. Krishna, J.M. Zadrozny, C.M. Brown, J.R. Long, Science 335 (2012) 1606, http://dx.doi.org/10.1126/science.1217544.
[31] A.L. Myers, J.M. Prausnitz, AIChE J. 11 (1965) 121, http://dx.doi.org/10.1002/aic.690110125.
[32] S. Furmaniak, S. Koter, A.P. Terzyk, P.A. Gauden, P. Kowalczyk, G. Rychlicki, Phys. Chem. Chem. Phys. 17 (2015) 7232, http://dx.doi.org/10.1039/C4CP05498A.
[33] M. Murthi, R.Q. Snurr, Langmuir 20 (2004) 2489, http://dx.doi.org/10.1021/la035556p.
[34] V. Krungleviciute, A.D. Migone, M. Pepka, Carbon 47 (2009) 769, http://dx.doi.org/10.1016/j.carbon.2008.11.036.
[35] O. Talu, Adv. Colloid Interface Sci. 76–77 (1998) 227, http://dx.doi.org/10.1016/S0001-8686(98)00048-7.
[36] G. Vidali, G. Ihm, H.-Y. Kim, M.W. Cole, Surf. Sci. Rep. 12 (1991) 135, http://dx.doi.org/10.1016/0167-5729(91)90012-M.